Electronic Supplementary Information

Mechanism of the Large Second Harmonic Generation Enhancement Activated by the Zn^{2+} Substitution

Miriding Mutailipu, [a,b] Zhi Li, [a] Min Zhang, [*a] Dianwei Hou, [a,b]

Zhihua Yang, [a] Bingbing Zhang,[a] Hongping Wu [a] and Shilie Pan [*a]

[a] Key Laboratory of Functional Materials and Devices for Special Environments, Xinjiang Technical Institute of Physics & Chemistry, Chinese Academy of Sciences; Xinjiang Key Laboratory of Electronic Information Materials and Devices, 40-1 South Beijing Road, Urumqi 830011, China

[b]University of the Chinese Academy of Sciences, Beijing 100049, China

*Corresponding authors, E-mails: zhangmin@ms.xjb.ac.cn; slpan@ms.xjb.ac.cn

1. Results and Discussion

1.1. Synthesis and thermal behavior

The polycrystalline samples of $Sr_2ZnSi_2O_7$ and $Sr_2MgSi_2O_7$ for the measurement of thermal behavior were characterized by powder XRD (Fig. S3), which illustrates that those samples are pure phase without impurity. The TG and DSC curves of those samples are shown in Fig. S4. It is obvious that there are no any endothermic peakson each DSC curve and no weight loss on their TG curves within the region from 40 to 1400 °C, which shows that the melting temperature of both compounds are higher than 1400°C. The results guide us to use the flux method to obtain the single crystals.

1.2. Description of the structure

Single-crystal X-ray diffraction data show that $Sr_2ZnSi_2O_7$ and $Sr_2MgSi_2O_7$ crystallize in a tetragonal crystal system with a noncentrosymmetric space group of $P\bar{4}2_1m$ (No. 113). Since $Sr_2ZnSi_2O_7$ and $Sr_2MgSi_2O_7$ are isostructural, only the structure of $Sr_2ZnSi_2O_7$ will be discussed in details as a representation.

In the asymmetric unit of $Sr_2ZnSi_2O_7$, Sr, Zn, Si, O each occupies one, one, one and three crystallographically unique positions, respectively. The structure of $Sr_2ZnSi_2O_7$ is shown in Fig. S1, which can be seen as the structure consisting of $[ZnSi_2O_7]_\infty$ layers with the Sr atoms locating between these layers to balance the charge and holding the layers together through coordination with the O atoms.

In their structures, the Si and Zn (or Mg) atoms are four-coordinated to form AO_4 (A= Si, Zn and Mg) tetrahedra. The two SiO_4 tetrahedra are further connected by sharing an O atom to form the Si_2O_7 dimers (Fig. S1a). The ZnO_4 tetrahedra are linked with the Si_2O_7 dimers by vertex-sharing to form $^2_\infty[ZnSi_2O_7]$ layers (Fig. S1b) and stacked in the direction of *c* axis forming the final structures(Fig. S1c). In the SiO_4 tetrahedron, the bond distances range from 1.569(7) to 1.650(6) Å for Si-O, while all bonds of Zn-O in ZnO_4 tetrahedra are in the same distances of 1.925(5) Å. The bond valence calculations (BVSs) (Sr = 1.958, Zn = 2.201, O = 1.720 - 2.352, Si = 4.207) for $Sr_2ZnSi_2O_7$ show that the Sr, Zn, Si and O atoms are in oxidation states of +2, +2 +4 and -2, respectively, which are in agreement with reported compounds previously.

Moreover, two ZnO_4 tetrahedra and three SiO_4 groups are connected to construct a tunnel along *c* axis with the diameters of 3.8 Å (Fig. S1d), then eight-coordinated SrO_8 hexahedra are located in the tunnels.

1.3. Structure comparison among $Sr_2ZnSi_2O_7$ with α- and β-$Ba_2ZnSi_2O_7$.

It is worth comparing the structure of $Sr_2ZnSi_2O_7$ with those of α- and β-$Ba_2ZnSi_2O_7$.[1,2] There are some similarities in structure among them, all of those compounds contain topologically identical $^2_\infty[ZnSi_2O_7]$ layers (Figs. S1c, S2a and S2c) and Sr(or Ba) atoms locating between these layers to constitute the network structures. There are also some differences among three crystal structures with same molecular formula, and these differences are characterized as the following points: firstly, Si_2O_7 and ZnO_4 as the fundamental building blocks (FBBs) of $[ZnSi_2O_7]_\infty$ layers, are alternately parallelly arranged to form a layer for α and β-$Ba_2ZnSi_2O_7$ (Figs. S2a and S2c). But for $Sr_2ZnSi_2O_7$, the adjacent Si_2O_7 groups are perpendicular to each other in a regular manner (Fig. S2c). Secondly, the tunnels composed of two ZnO_4 unites and two Si_2O_7 groups adopt different arrangements, which is shown in Fig. S2c (A for $Sr_2ZnSi_2O_7$, B for α-$Ba_2ZnSi_2O_7$, C for β-$Ba_2ZnSi_2O_7$) and there are one, one and two Sr (or Ba) atoms located in the tunnels for three compounds, respectively. Thirdly, there is no shared-oxygen O atom between two ZnO_4 units in chains Ⅰ and Ⅱ for $Sr_2ZnSi_2O_7$ and α-$Ba_2ZnSi_2O_7$, respectively. While for chain Ⅲ in β-$Ba_2ZnSi_2O_7$, there is single atom between two ZnO_4 groups(Fig. S2d), which may lead link more closely in β-$Ba_2ZnSi_2O_7$ than another.

1.4 Electronic structure

Electronic states near the band gap are important for the optical properties, so the electronic structure was analyzed. The density of states (DOS) and the partial density of states (PDOS) of $Sr_2MSi_2O_7$ (M = Zn and Mg) are shown in Fig. S8. The upper region of the valence band (VB) is mainly occupied by the O 2p orbitals for $Sr_2MSi_2O_7$ (M = Zn and Mg). The bottom of the conduction band (CB) mainly consists of the Zn 4s orbitals for $Sr_2ZnSi_2O_7$ and Sr 5s for $Sr_2MgSi_2O_7$. Hence, for $Sr_2ZnSi_2O_7$, the band gap is determined by the O and Zn atoms, and the band gap of

$Sr_2MgSi_2O_7$ is dependent on the O and Sr atoms. In contrast to the 3*s* orbitals of Mg, the 4*s* orbitals of Zn is more spatially extended. The spatially extended 4*s* orbitals will enhance the *sp* hybridization between Zn and O. This enhanced *sp* hybridization has two sequences: (1) it will enhance the bandwidth of 4*s* orbitals and reduce the band gap; (2) it will enhance the inter-band dipole and inter-band transition induced by laser light.

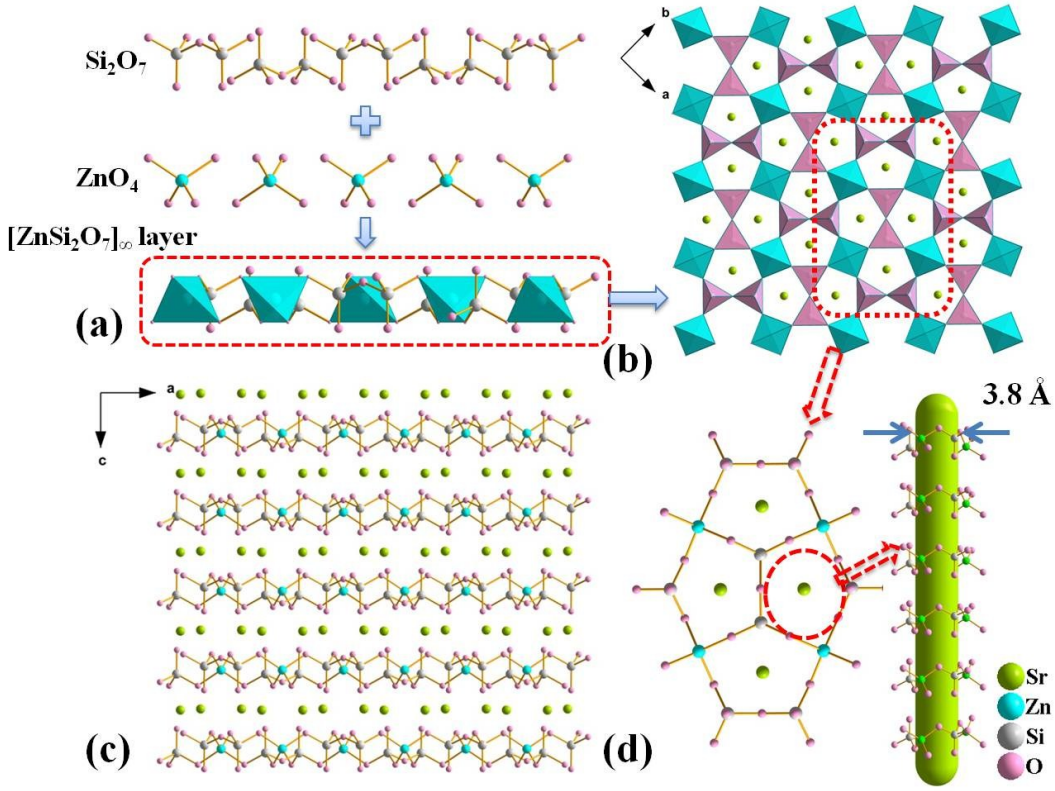

Fig. S1. Structure of $Sr_2ZnSi_2O_7$. (a) The ZnO_4 tetrahedra and Si_2O_7 dimers. (b) The $^2_\infty[ZnSi_2O_7]$ layer in the structure viewed along the *c* axis.(c) Crystal structure of $Sr_2ZnSi_2O_7$ viewed in the direction of *b* axis. (c) The $^2_\infty[ZnSi_2O_7]$ layer in the structure viewed along the *c* axis. (d) The tunnel in $Sr_2ZnSi_2O_7$. The ZnO_4 and SiO_4 groups are shown in turquoise and rose, respectively.

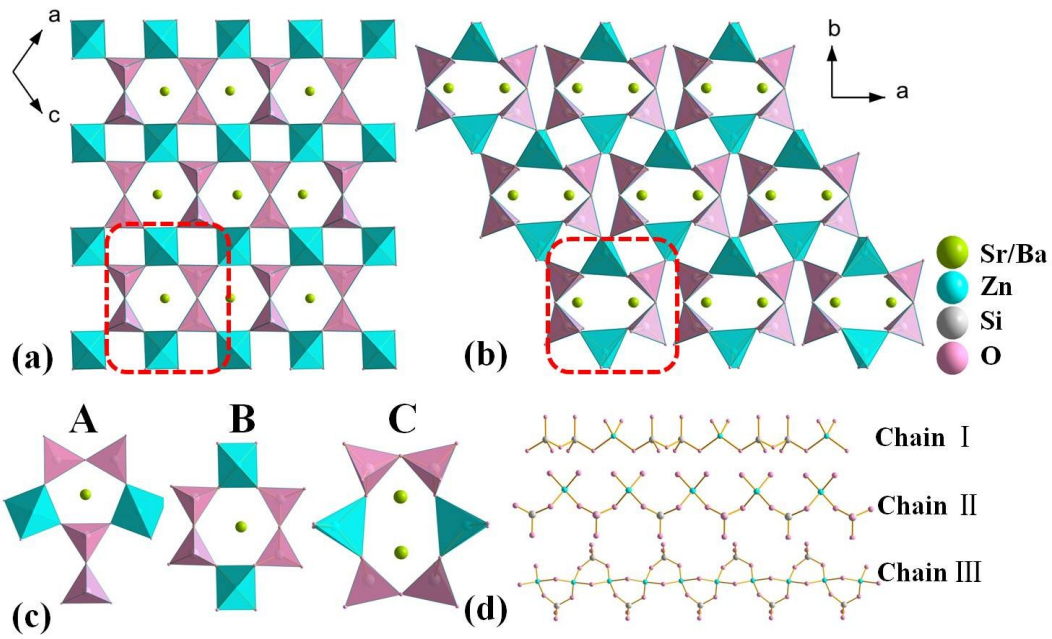

Fig. S2. The $^{2}_{\infty}[ZnSi_2O_7]$ layers in α-$Ba_2ZnSi_2O_7$ viewed along the *b* axis (a) and in β-$Ba_2ZnSi_2O_7$ viewed along the *c* axis (b). The tunnels of three compound (c). chains Ⅰ, Ⅱ and Ⅲ for three compound (d). The ZnO_4 and SiO_4 groups are shown in turquoise and rose, respectively.

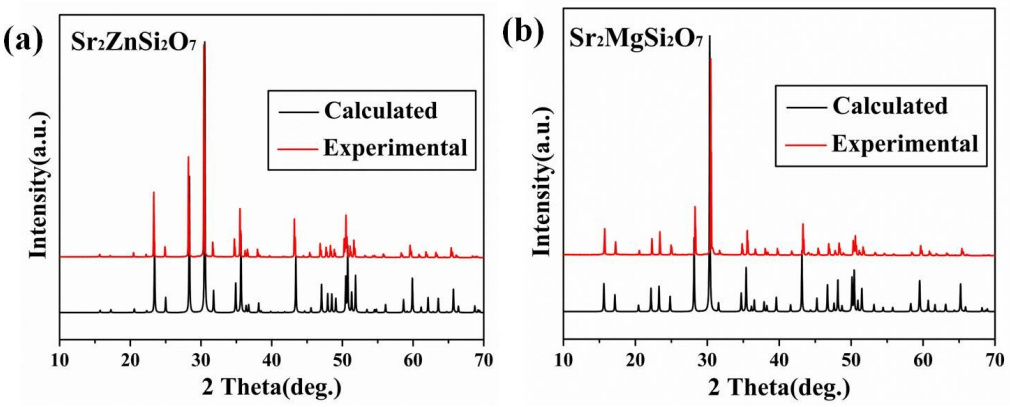

Fig. S3. Experimental and calculated XRD patterns of $Sr_2ZnSi_2O_7$ (a) and $Sr_2MgSi_2O_7$ (b).

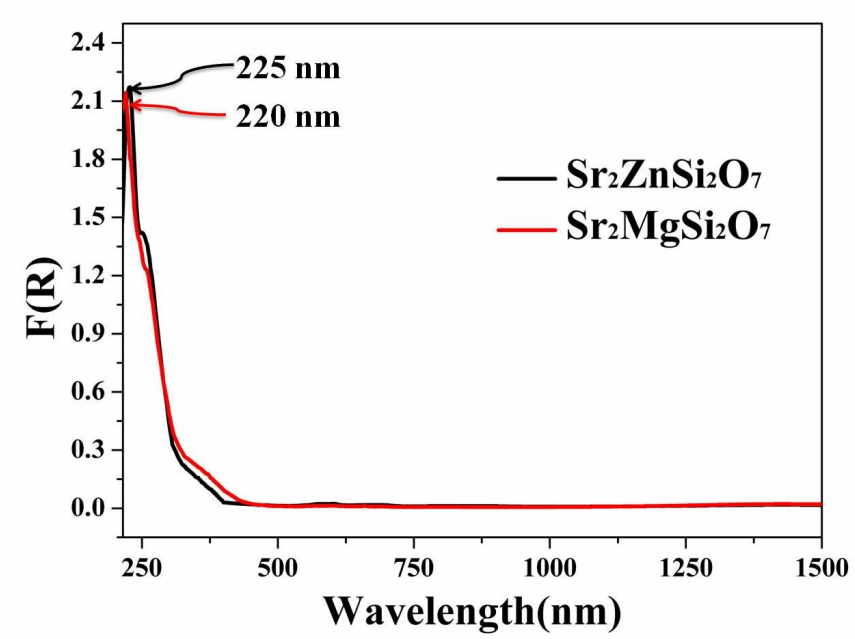

Fig. S4. The UV-vis-NIR diffuse reflectance spectra of $Sr_2ZnSi_2O_7$ and $Sr_2MgSi_2O_7$.

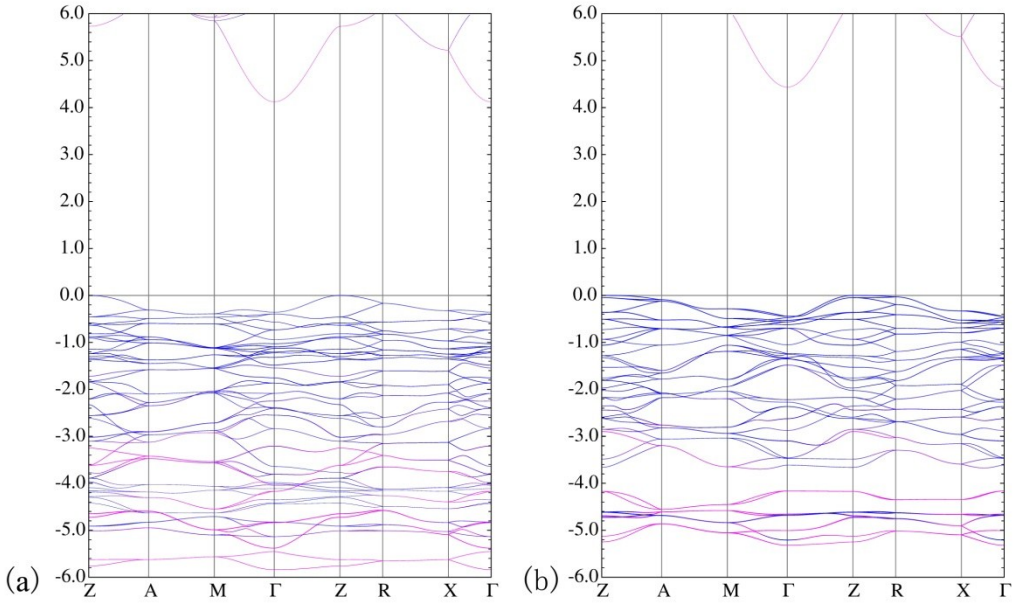

Fig. S5. Calculated band structures of $Sr_2ZnSi_2O_7$ (a) and $Sr_2MgSi_2O_7$(b). The weight of 3s-orbitals of Si is in red, and the weight of 3p-orbitals of O is in blue.

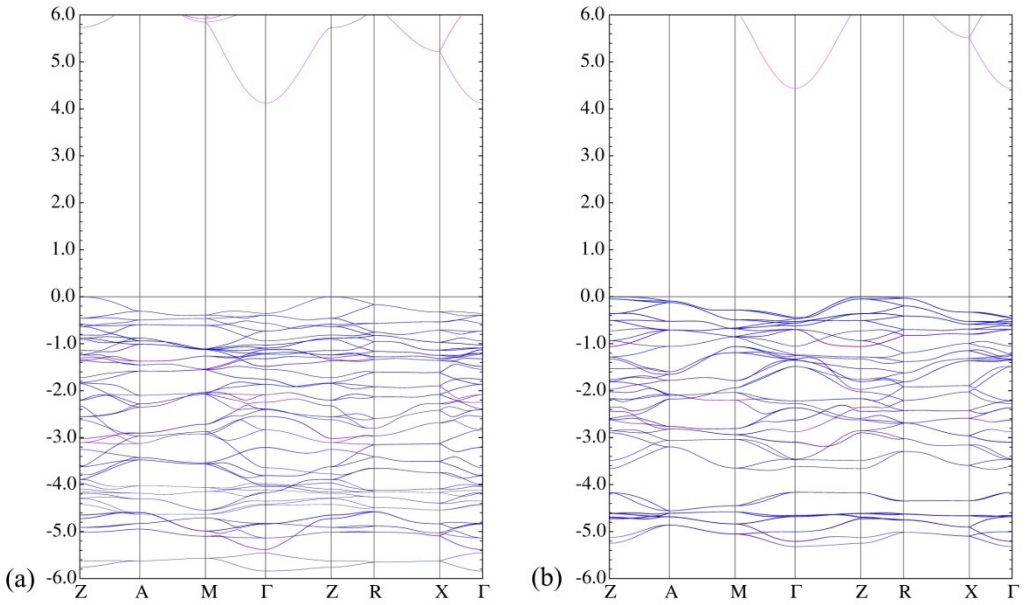

Fig. S6. Calculated band structures of $Sr_2ZnSi_2O_7$ (a) and $Sr_2MgSi_2O_7$(b). The weight of 3s-orbitals of Sr is in red, and the weight of 3p-orbitals of O is in blue.

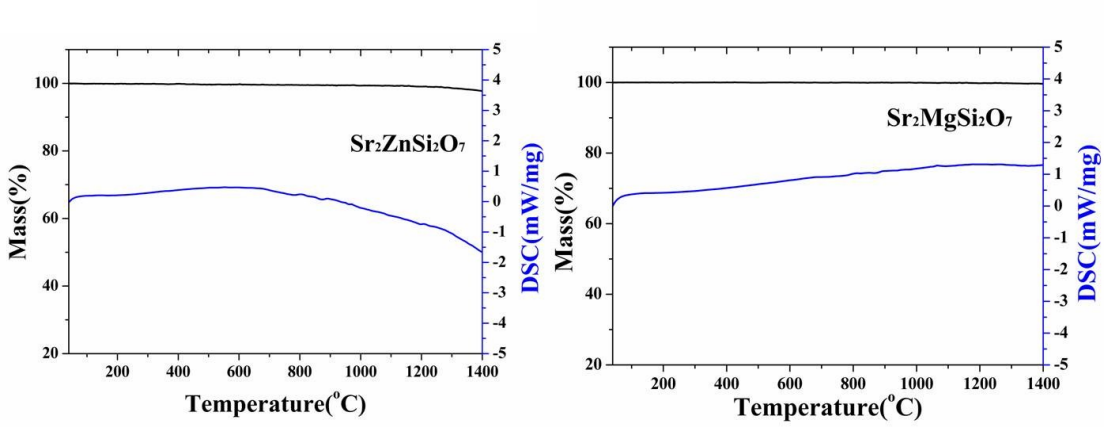

Fig. S7. The TG and DSC curves of $Sr_2ZnSi_2O_7$ and $Sr_2MgSi_2O_7$.

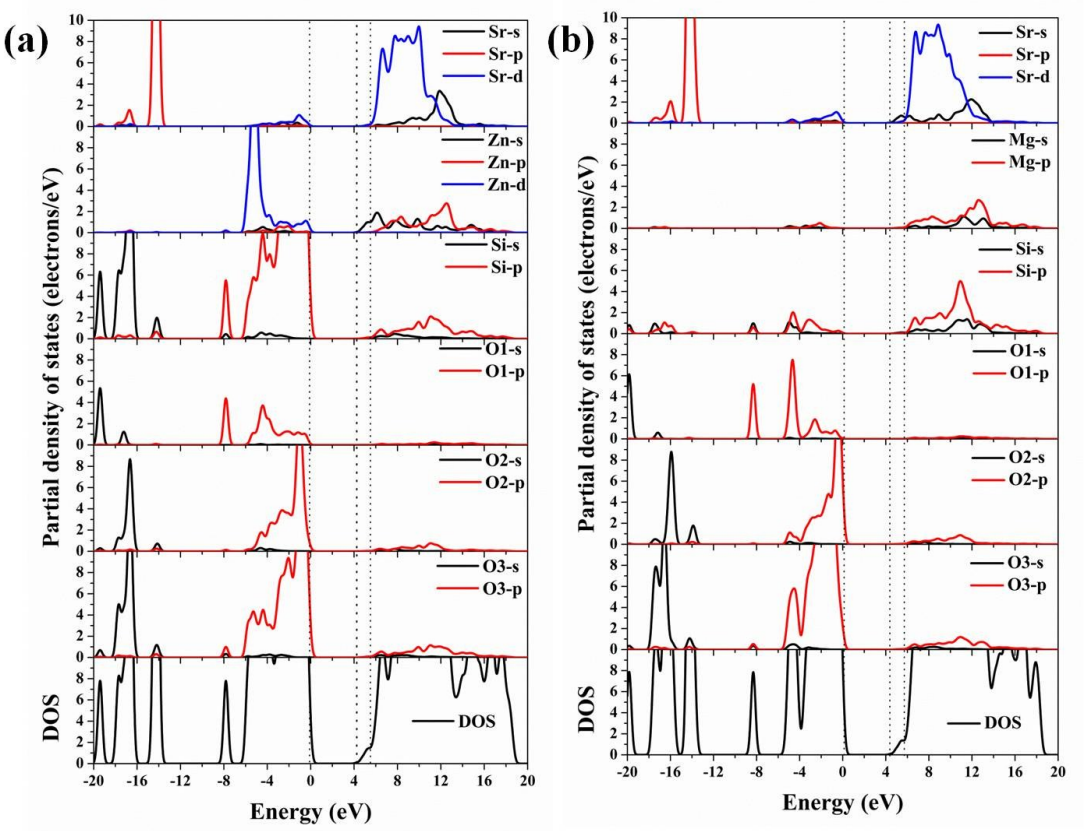

Fig. S8. The density of states and the partial density of states of $Sr_2ZnSi_2O_7$ (a) and $Sr_2MgSi_2O_7$ (b).

Table S1. Crystallographic data for $Sr_2ZnSi_2O_7$ and $Sr_2MgSi_2O_7$.[3]

empirical formula	$Sr_2ZnSi_2O_7$	$Sr_2MgSi_2O_7$[3]
Formula weight	408.79	367.72
Crystal system	Tetragonal	Tetragonal
space group	$P\bar{4}2_1m$ (No. 113)	$P\bar{4}2_1m$ (No. 113)
a (Å)	7.956 (2)	7.9957(10)
b (Å)	7.956 (2)	7.9954(10)
c (Å)	5.136(3)	5.1521(9)
Z	2	2
volume (Å^3)	325.1 (2)	329.54(8)
density (calcd) (g/cm^3)	4.176	3.707
abs coeff (mm^{-1})	20.366	-
F(000)	380	344
cryst size (mm^3)	0.19 ×0.15 ×0.10	0.08×0.07×0.06
the range for data collection (deg)	3.62 to 27.46	-
index ranges	$-10 \le h \le 10$, $-4 \le k \le 10$, $-6 \le l \le 6$	-
reflns collected/unique	1978 / 416 [*R*(int) = 0.0259]	-
completeness to $\theta = 27.46°$	100 %	-
data/restraints/param	416 / 0 / 35	-
GOF on F^2	1.192	-
final *R* indices [$F_o^2 > 2\sigma(F_o^2)$][a]	*R*1 = 0.0277, *wR*2 = 0.0715	-
R indices (all data) [a]	*R*1 = 0.0297, *wR*2 = 0.0727	-
extinction coeff	0.010(3)	-
largest diff peak and hole (e/Å^3)	0.637 and -1.288	-

[a] $R_1 = \Sigma||F_o| - |F_c||/\Sigma|F_o|$ and $wR_2 = [\Sigma w(F_o^2 - F_c^2)^2 / \Sigma w F_o^4]^{1/2}$ for $F_o^2 > 2\sigma(F_o^2)$ and $w^{-1} = \sigma^2(F_o^2) + (0.0254P)^2 + 0.49P$ where $P = (F_o^2 + 2F_c^2)/3$.

Table S2. Atomic coordinates equivalent isotropic displacement parameters and bond valence Sum (BVS) for $Sr_2ZnSi_2O_7$[a] and $Sr_2MgSi_2O_7$.[3]

Atoms	*x*	*y*	*z*	U_{eq}(Å^2)	BVS
		$Sr_2ZnSi_2O_7$			
Sr	0.3327(1)	0.8327(1)	0.0069(2)	0.012(1)	1.958
Zn	0.0000	1.0000	0.5000	0.012(1)	2.201
Si	0.1365(3)	0.6365(3)	0.4498(6)	0.026(1)	4.207
O1	0.5000	1.0000	-0.3475(19)	0.018(2)	2.352
O2	0.1385(6)	0.6385(6)	-0.2446(12)	0.017(2)	1.720
O3	0.0755(7)	0.8096(7)	0.3005(11)	0.024(1)	2.025
		$Sr_2MgSi_2O_7$[2]			
Sr	0.3345(5)	0.1655(5)	0.5077(1)	-	1.958
Mg	0.0000	0.0000	0.0000	-	2.041
Si	0.1387(2)	0.3613(2)	0.9438(4)	-	4.260
O1	0.5000	0.0000	0.1603(15)	-	2.184
O2	0.1396(6)	0.3604(6)	0.2528(10)	-	1.509
O3	0.0793(5)	0.1915(5)	0.8034(7)	-	1.950
Sr	0.3345(5)	0.1655(5)	0.5077(1)	-	1.958

Table S3. Selected bond lengths (Å) for $Sr_2ZnSi_2O_7$ and $Sr_2MgSi_2O_7$.[3]

Selected bond	Bond lengths	Selected bond	Bond lengths
	$Sr_2ZnSi_2O_7$		
Sr(1)-O(2)	2.538(7)	Zn(1)-O(3)$^{\#7}$	1.925(5)
Sr(1)-O(3)	2.548(5)	Zn(1)-O(3)	1.925(5)
Sr(1)-O(3)$^{\#1}$	2.548(5)	Zn(1)-O(3)$^{\#8}$	1.925(5)
Sr(1)-O(1)	2.619(7)	Zn(1)-O(3)$^{\#9}$	1.925(5)
Sr(1)-O(2)$^{\#2}$	2.732(5)	Si(1)-O(2)$^{\#11}$	1.569(7)
Sr(1)-O(2)$^{\#3}$	2.732(5)	Si(1)-O(1)$^{\#10}$	1.623(5)
Sr(1)-O(3)$^{\#2}$	2.740(6)	Si(1)-O(3)	1.650(6)
Sr(1)-O(3)$^{\#4}$	2.740(6)	Si(1)-O(3)$^{\#1}$	1.650(6)
	$Sr_2MgSi_2O_7$[3]		
Sr(1)-O(3)	2.538	Mg(1)-O(3)	1.942
Sr(1)-O(3)	2.548	Mg(1)-O(3)	1.942
Sr(1)-O(2)	2.548	Mg(1)-O(3)	1.942
Sr(1)-O(1)	2.619	Mg(1)-O(3)	1.942
Sr(1)-O(2)	2.732	Si(1)-O(2)	1.592
Sr(1)-O(2)	2.732	Si(1)-O(3)	1.610
Sr(1)-O(3)	2.740	Si(1)-O(3)	1.610
Sr(1)-O(3)	2.740	Si(1)-O(1)	1.658

Table S4. Calculated SHG effect of $Sr_2ZnSi_2O_7$ and $Sr_2MgSi_2O_7$

Compounds	Calculated (pm/V)
$Sr_2ZnSi_2O_7$	0.29
$Sr_2MgSi_2O_7$	0.07

Table S5. Calculated band-resolved results of $Sr_2ZnSi_2O_7$ and $Sr_2MgSi_2O_7$

Compounds	VE process	VH process
$Sr_2ZnSi_2O_7$	98.02%	71%
$Sr_2MgSi_2O_7$	1.98%	29%

References and Notes

(1) Kaiser, J. W.; Jeitschko, W.; Krist, Z. *New. Cryst. St.* **2002**, *217*, 25.

(2) Lin, J. H.; Lu, G. X.; Du, J.; Su, M. Z.; Loong, C. K.; Richardson, J. W. *J. Phys. Chem. Sol.* **1999**, *60*, 975.

(3) Kimata, M. Z. *Kristallogr*. **1983**, *163*, 295.